High-T_c Dual-SQUIDs With Graphoepitaxial Step-Edge Junctions

M. I. Faley, V. Yu. Slobodchikov, Yu. V. Maslennikov, V. P. Koshelets, and R. E. Dunin-Borkowski

Abstract—**The microstructural and noise properties of serially connected high-T_c dc superconducting quantum interferometer devices (high-T_c dc SQUIDs) with step-edge Josephson junctions are studied. It is shown that the implementation of novel graphoepitaxial step-edge Josephson junctions on buffered MgO substrates helps to overcome poor reproducibility of conventional step-edge high-T_c Josephson junctions due to the self-arranged growth of two identical [100]-tilted 45° grain boundaries over a wide range of step heights. The use of such Josephson junctions in two serially connected SQUIDs that are directly coupled to a common pickup loop in a dual-SQUID configuration with current biasing of the individual SQUIDs results in a doubling of voltage swings and an improvement in magnetic field resolution of the sensors.**

Index Terms—**High-temperature superconductors, Josephson junctions, magnetic sensors, SQUIDs.**

I. INTRODUCTION

THE UNRIVALED sensitivity of direct current superconducting quantum interferometer devices (DC SQUIDs) to magnetic flux makes them useful for applications such as biomagnetic measurements, geomagnetic surveys and non-destructive evaluations (see [1] and references therein). Sources of magnetic signals in these studies often have a dipole-like behavior. In order to harvest the maximum information from an object, dense arrays of relatively small magnetic field sensors each having the highest possible sensitivity and placed as close as possible to the object are required [2]. SQUIDs that are based on high-T_c superconductors such as $YBa_2Cu_3O_{7-x}$ (YBCO) and made without a superconducting flux transformer can be placed within ~15 μm from the outer side of a cryostat [3]. The magnetic field resolution of SQUIDs can be improved by using a superconducting flux transformer, which concentrates magnetic flux from a larger area into the SQUID loop. SQUIDs that are directly coupled to 8×8 mm^2 single turn pick-up loops can also be mounted on a cooled sapphire rod in the vacuum region of a liquid nitrogen cryostat resulting in a typical separation of about 3 mm between the SQUID and the room temperature side of the cryostat [4]. High-T_c SQUIDs with multilayer flux

transformer, in a flip-chip configuration are usually encapsulated in an approximately 1 cm thick capsule and cooled in liquid nitrogen at a distance of about 15 mm between the pickup loop of the flux transformer and the room temperature side of the cryostat [5]. There is a need for SQUID magnetometers, for both biomagnetic measurements and non-destructive evaluation that can be placed in a similar way to a directly coupled magnetometer but provide better magnetic field resolution.

A serial connection of two SQUIDs that are directly coupled to a common pick-up loop (dual-SQUID) can enhance the peak-to-peak value of the output voltage (voltage swing) of the sensor and provide a reduction of its intrinsic noise by a factor of $1/\sqrt{2}$ [6]. The dual-SQUID configuration has been tested with step-edge Josephson junctions, but typically only one of two SQUIDs was used and a magnetic field resolution of ~60 fT/$\sqrt{Hz}$ at 10 kHz and 77 K was achieved [7]. More SQUIDs can be connected in series with the same pick-up loop, choosing the two best SQUIDs and improving the magnetic field noise level of the two-SQUID magnetometer to ~33 fT/$\sqrt{Hz}$ at 1 kHz and 77 K [8]. In this paper, we report the preparation and characterization of high-T_c dual-SQUID magnetometers made with graphoepitaxial step-edge Josephson junctions [9]–[11], as well as the modification of the readout electronic circuit, which can be used for simultaneous operation of both SQUIDs in such sensors.

II. EXPERIMENTAL DETAILS

A. Graphoepitaxial Step-Edge Josephson Junctions

Samples were prepared on single crystal MgO (100) substrates of size 10 mm $\times$ 10 mm $\times$ 1 mm with their edges oriented along the [100] and [010] directions. The surface of the substrate was Ar ion beam etched using a photolithography mask to prepare steps on the substrate surface with a height in the range of 0.5–1 μm and with a slope angle of the step edge of ~45°. A side-view scanning electron microscopy (SEM) image of a 45° step on an MgO (100) substrate is shown in Fig. 1.

The best reproducibility of Josephson junctions, the largest voltage swing and the lowest noise values of the SQUIDs were achieved for a step height of approximately 0.6 μm. After etching, the photoresist mask was stripped using acetone in an ultrasonic bath and the substrate was additionally cleaned using methanol. A second ion beam milling step was used for cleaning of the surface [12] to remove residuals of resputtered material such as fences, which appeared at the top corners of the steps during the first ion beam milling procedure, as well as to create a texture in the form of linear trenches along the (100) and (010) planes of the MgO substrate on the surface (see Fig. 2).
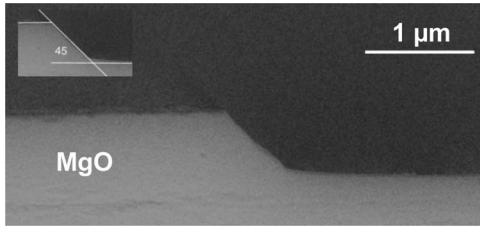
Fig. 1. Side-view SEM image of an ion milled 45° step edge on an MgO substrate. The inset in the top left corner of the picture shows the slope angle of the edge surface relative to the substrate (001) plane. The image was obtained by using a cut of the sample perpendicular to the step.
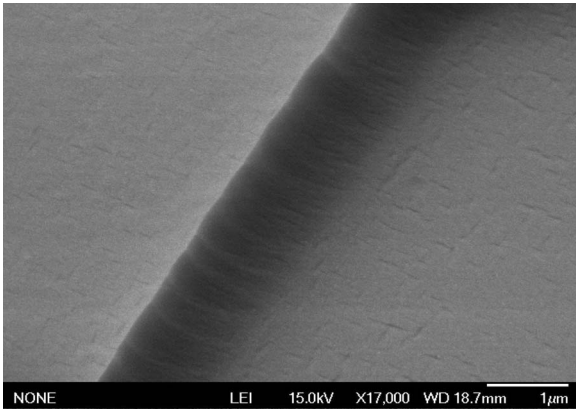

Fig. 2. SEM image of the step edge with a surface texture made by a second ion milling procedure. The bottom corner of the step is smoothed due to the simultaneous effects of the angular dependence of the ion beam milling and the partial redeposition of etched material.

Alternatively, the texture can be made by depositing an approximately 10 nm thick homoepitaxial MgO film [13]. However, up to now this has not led to any significant advantages in the electron transport properties of the Josephson junctions when compared to the results obtained with texturing by ion beam milling and this method was not used in the present work. The disadvantage of using of ion beam milling for texturing is that the shape of the bottom part of the step edge is changed by the simultaneous effects of the angular dependence of the ion beam milling and the partial redeposition of the etched material: the bottom corner of the step edge then becomes partially rounded. On the other hand, ion beam texturing is a much simpler procedure compared to the deposition of a homoepitaxial MgO film. Rounded bottom corners of steps on MgO substrates have been obtained before by another group (see [12] and references therein). However, in that case the surface texture was not observed. The critical current of the described Josephson junctions is essentially independent of the height of the step edge, but the resistance of the junctions has a tendency of decreasing with the height of the step and there is an increase of rounding of the bottom corner of the step after a long ion beam etching procedure.

The steps were covered by an epitaxial double buffer layer made from a seed layer and a blocking layer [9], [11]. The time for transportation of the substrates from the ion beam machine to the sputtering machine was about 1 minute. The texture was used to achieve graphoepitaxial growth of an approximately 10 nm thick non-superconducting YBCO seed film, resulting in
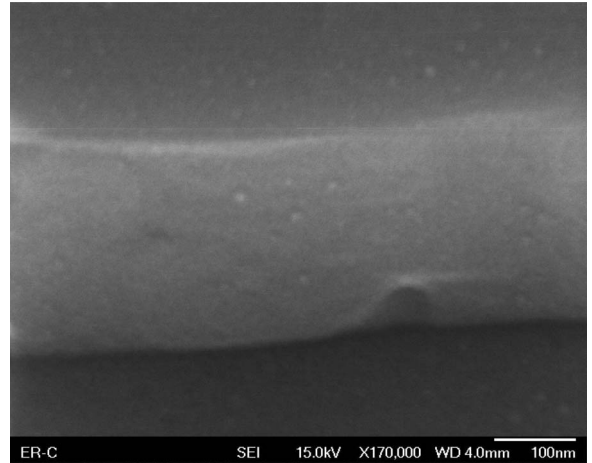

Fig. 3. SEM image of the step edge covered by a graphoepitaxial YBCO/STO/ YBCO heterostructure. The image was obtained normal to the substrate (001) plane. The top corner of the step edge is seen as a bright line in the top part of the image, whereas the bottom corner of the step edge is dark and is in the bottom part of this image.

an in-plane orientation of the a-axis or b-axis of the YBCO seed film normal to both grain boundaries of the step edge junction. An epitaxial 30 nm thick blocking layer of $SrTiO_3$ (STO) was deposited above the YBCO seed layer to avoid contamination of the subsequent YBCO film by impurities from the MgO substrate [14]. The YBCO and STO films were deposited by high-oxygen-pressure magnetron sputtering from stoichiometric polycrystalline targets [15], [16]. Two [100]-tilted grain boundaries with 45° misorientations were formed at the top and bottom corners of the step edge and propagated through all 3 layers of the YBCO/STO/YBCO heterostructure [11]. These 45° grain boundaries, one in the top part of the step and another in the bottom part of the step, as well as a flat single crystal region between them were clearly visible in high resolution SEM images (see Fig. 3). For strongly rounded bottom corner, additional grains of YBCO film were observed in the edge region.

The top YBCO film had a thickness of $\sim$200 nm, $T_c \sim 93$ K and critical current density ~ 5 MA/cm^2. YBCO deposition was followed by the sputtering of a 5 nm thick platinum layer for overall passivation and to achieve a better electrical contact to the contact pads.

Josephson junctions were formed by photolithography by using a mask from a deep-UV AZ TX1311 photoresist and ion beam etching of ~ 2 μm wide bridges across the step-edge. The typical resistance of each junction was $\sim$10 Ω and the critical current was ~ 30 μA at 77 K. Electrical contacts were made by using 100 nm thick Ag contact pads and Ag wires pressed onto the contact pads by pieces of indium.

B. Dual-SQUID and Readout Electronics

The magnetometers were realized with two serially connected DC SQUIDs galvanically (directly) connected together by a common pick-up loop (see Figs. 4 and 5). We denote "SQUID" as the SQUID structure alone without the pick-up loop. Two SQUIDs combined with a common pickup loop will be referred to as a "dual-SQUID magnetometer." "SQUID magnetometer" refers to a SQUID with pick-up loop. Each individual SQUID had $\sim$140 μm long SQUID loop having an inductance L_S of
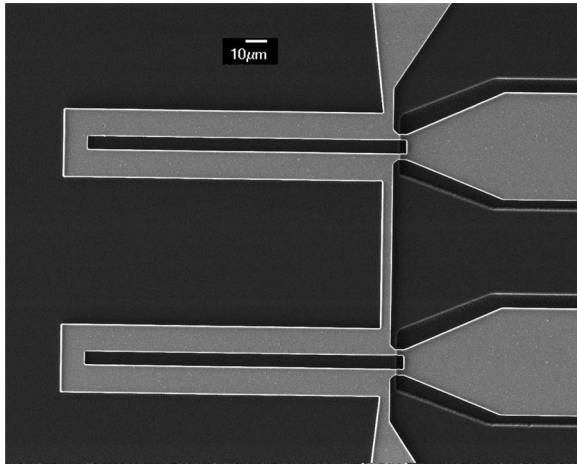
Fig. 4. SEM image of the inner part of a dual-SQUID with two dc SQUIDs each having two 2-μm-wide step-edge Josephson junctions and a 140-μm-long SQUID loop with an inductance of approximately 100 pH.
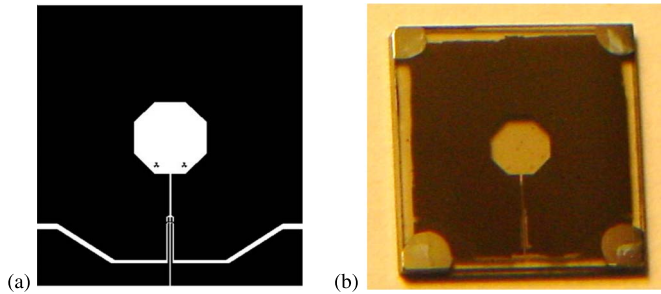

Fig. 5. (a) Sketch and (b) photo of a complete high-T_c dual-SQUID magnetometer with four contact pads at the corners of a 10 mm × 10 mm MgO substrate. One of the upper contact pads, connected to a common pickup loop, was used to inject an additional current to the SQUID, which have the largest bias current value.

$\sim$100 pH. Together with a 7 mm × 8 mm pick-up loop of inductance $L_{pu} \sim 4$ nH, the field-to-flux coefficients of the SQUID magnetometer and the dual-SQUID magnetometer were $\sim$5 nT/Φ_0, corresponding to an effective area of $\sim$0.4 mm^2. Peak-to-peak voltage swings of each of the SQUIDs were $\sim$40 μV at 77 K. The estimates of the inductances were made with the help of the software package 3D-MLSI [17].[1]

There was a small spread of critical currents of the Josephson junctions $\delta I_c/I_c \sim 10\%$, which resulted in a difference in the optimal bias currents of the SQUIDs: one SQUID had a bias current of $\sim$55 μA, while another SQUID had a bias current of $\sim$53 μA. In order to compensate for this difference, we have proposed a simple electrical circuit, which is shown schematically in Fig. 5. The main part of the bias current for both SQUIDs was formed by the voltage V_B and resistances $R_1 \approx 25$ kΩ and $R_4 \approx 25$ kΩ. The capacitances C ≈ 0.1 μF prevent the flow of the bias current through the primary coil of the matching transformer. A small correction of the bias current for the bottom SQUID was provided by the injection of an additional current into the pick-up loop via the resistances R_2 and R_3. We observed that the point where this additional current was injected into the pick-up loop was not essential: instead of connecting

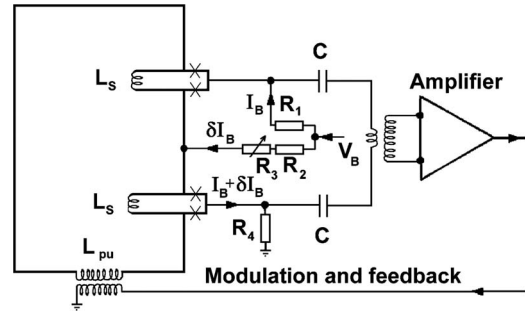[1][Online]. Available: http://vm.cs.msu.ru/sotr/vmhap/3dmlsi/3dmlsi.htm

Fig. 6. Schematic representation of a dual-SQUID connected with circuits for current biasing, voltage readout, modulation, and feedback.
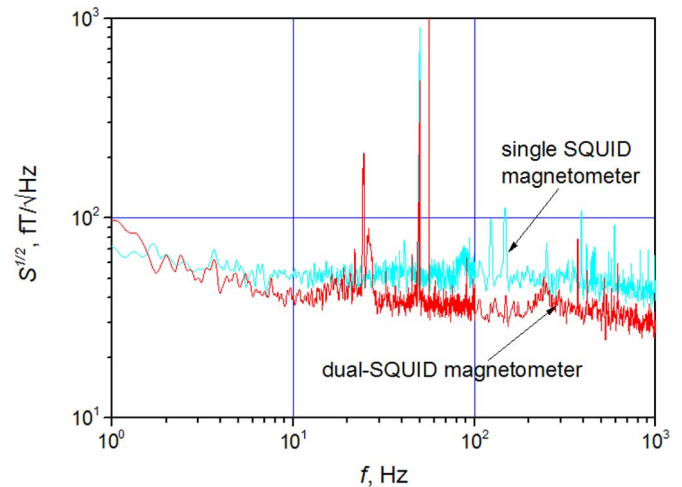

Fig. 7. Noise spectra $S^{1/2}(f)$ of one of the SQUIDs and of the dual-SQUID magnetometer measured with the same pickup loop, taken with ac biasing. The top curve corresponds to the noise measured with an individual SQUID connected to the pickup loop. The bottom curve represents the noise of the dual-SQUID magnetometer.

the resistors R_2 and R_3 between the SQUIDs as shown schematically in Fig. 6 and in [6], we connected them to the pick-up loop at one of the two upper corners of the substrate, as shown in Fig. 4. Our magnetometer can be mounted on the cold finger of a cryocooler or in a cryostat, like a standard surface mounted electronic component. The biasing of individual SQUIDs was foreseen in [6], but to our knowledge, was never used.

With an optimal value $R_2 + R_3 \approx 280$ kΩ, the voltage swings of the dual-SQUID magnetometer were increased to approximately 80 μV at 77 K. Without the proposed bias current injection, the peak-to peak voltage swings of the dual-SQUID magnetometer were $\sim$60 μV at 77 K.

The measurements of intrinsic noise of the magnetometers were performed with sensors immersed in liquid nitrogen in a magnetic shield constructed from 3 cylinders of μ-metal and one superconducting cylinder made from a 100 μm thick YBCO film. The spectral densities of recalculated to the input noise of output signals of the system with SQUID magnetometers and with dual-SQUID magnetometer are shown in Fig. 7. A decrease in white noise from the white noise of a single SQUID magnetometer of $\sim$50 fT/$\sqrt{\text{Hz}}$ to the noise of the dual-SQUID magnetometer $\sim$35 fT/$\sqrt{\text{Hz}}$ at frequencies above 100 Hz and 77 K was observed.

III. Discussion

The reproducibility of Josephson junctions and the high value of their $I_c R_n$ product are essential for achieving large voltage swings and low white noise values of single SQUID magnetometers and dual-SQUID magnetometers. Graphoepitaxial Josephson junctions are sufficiently reproducible, they demonstrate good superconducting properties and they are relatively cheap. The disadvantage of this technology is that such junctions are sophisticated and, at least during optimization of their technological parameters, there is a need for high resolution electron microscopy to control the orientation of the YBCO films on the step edge surface.

The effect of reducing the junction resistance by rounding of the bottom corner of the step can be associated with the appearance of additional grains at the bottom corner of the step having tilt of the c-axis of $\sim 34°$ relative to the (001) plane of MgO [18], [19]. The expected critical current density of $\sim 34°$ [100]-tilted grain boundaries is much higher than the critical current density of $45°$ [100]-tilted grain boundary at the top corner of the step. Then only one $45°$ [100]-tilted grain boundary at the top corner of the step edge contributes to the SQUID operation, with two times smaller resistance and voltage swing values compared to step edge junctions having two $45°$ [100]-tilted grain boundaries.

We have also observed that a small spread of the parameters of individual SQUIDs can be corrected by the injection of an additional current into the pick-up loop. In this case, not only a doubling of the voltage swings, but also a reduction of the white noise value can be achieved. For a larger difference of the bias currents of individual SQUIDs, the voltage swings of the dual-SQUID magnetometer can be increased to the value equal to the sum of the voltage swings of the individual SQUIDs, but the reduction in noise is less pronounced, if at all. The latter effect is probably due to non-optimal operation of the ac-bias SQUID electronics and can probably be corrected in future experiments. The developed dual-SQUIDs and corresponding electronic circuit possess sufficiently low intrinsic noise make them useful for biomagnetic measurements, geomagnetic surveys and non-destructive evaluations.

IV. Conclusion

The microstructural and noise properties of graphoepitaxial step edge Josephson junctions and high-T_c dual-SQUIDs have been studied. Novel graphoepitaxial step edge Josephson junctions on buffered MgO substrates have sufficient reproducibility and good superconducting parameters for the preparation of dual-SQUID magnetometers with high voltage swing value approximately 80 μV and low white noise values of approximately 35 fT$/\sqrt{}$Hz at 77 K. The investigated dual-SQUIDs with the proposed electronic circuit can be used for biomagnetic measurements, geomagnetic surveys and non-destructive evaluations.

References

[1] *Applied Superconductivity: Handbook on Devices and Applications*, vol. 2, P. Seidel Ed. Weinheim, Germany: Wiley, 2015.

[2] J. F. Schneiderman, "Information content with low- vs. high-Tc SQUID arrays in MEG recordings: The case for high-T_c SQUID-based MEG," *J. Neurosci. Methods*, vol. 222, pp. 42–46, Jan. 2014.

[3] T. S. Lee, Y. R. Chemla, E. Dantsker, and J. Clarke, "High-T_c SQUID microscope for room temperature samples," *IEEE Trans. Appl. Supercond.*, vol. 7, no. 2, pp. 3147–3150, Jun. 1997.

[4] F. Öisjöen *et al.*, "High-T_c superconducting quantum interference device recordings of spontaneous brain activity: Towards high-T_c magnetoencephalography," *Appl. Phys. Lett.*, vol. 100, 2012, Art. ID 132601.

[5] M. I. Faley *et al.*, "Magnetoencephalography using a multilayer high-T_c DC SQUID magnetometer," *Phys. Procedia*, vol. 36, pp. 66–71, 2012.

[6] R. H. Cantor and M. J. Burns, *Multiple SQUID Direct Signal Injection Device Formed on a Single Layer Substrate*, Patent US 5 767 043, Jun. 16, 1998.

[7] S. K. H. Lam *et al.*, "Low-noise single-layer YBa$_2$Cu$_3$O$_{7-x}$ dc superconducting quantum interference devices magnetometers based on step-edge junctions," *J. Appl. Phys.*, vol. 113, 2013, Art. ID 123905.

[8] C.-H. Wu, H.-C. Yang, J.-C. Chen, K.-L. Chen, and M. J. Chen, "Superconducting-quantum-interference-device array magnetometers with directly coupled pickup loop and serial flux dams," *J. Appl. Phys.*, vol. 100, 2006, Art. ID 064510.

[9] M. I. Faley, *Reproducible Step-Edge Josephson Junction*, Patent US 20 150 069 331, Mar. 12, 2015.

[10] M. I. Faley *et al.*, "High-T_c DC SQUIDs for magnetoencephalography," *IEEE Trans. Appl. Supercond.*, vol. 23, no. 3, pt. 1, 2013, Art. ID 1600705.

[11] M. I. Faley, D. Meertens, U. Poppe, and R. E. Dunin-Borkowski, "Graphoepitaxial high-T_c SQUIDs," *J. Phys., Conf. Ser.*, vol. 507, 2014, Art. ID 042009.

[12] E. E. Mitchell and C. P. Foley, "YBCO step-edge junctions with high IcRn," *Supercond. Sci. Technol.*, vol. 23, 2010, Art. ID 065007.

[13] C. A. Copetti *et al.*, "Graphoepitaxy of CeO$_2$ on MgO and its application to the fabrication of 45° grain boundary Josephson junctions of YBa$_2$Cu$_3$O$_{7-x}$," *J. Appl. Phys.*, vol. 78, no. 8, pp. 5058–5061, Oct. 15, 1995.

[14] Z. Hao, Y. Wu, Y. Enomoto, K. Tanabe, and N. Koshizuka, "Microstructure and magnesium diffusion in YBa$_2$Cu$_3$O$_{7-\delta}$ films on bicrystal MgO substrates," *J. Appl. Phys.*, vol. 91, no. 11, pp. 9251–9254, Jun. 1, 2002.

[15] U. Poppe *et al.*, "Low-resistivity epitaxial YBa$_2$Cu$_3$O$_{7-x}$ thin films with improved microstructure and reduced microwave losses," *J. Appl. Phys.*, vol. 71, pp. 5572–5578, 1992.

[16] M. I. Faley and U. Poppe, *Sputtering Sources for High-Pressure Sputtering With Large Targets and Sputtering Method*, Patent US 20 130 199 924, Aug. 8, 2013.

[17] M. M. Khapaev, M. Y. Kupriyanov, E. Goldobin, and M. Siegel, "Current distribution simulation for superconducting multi-layered structures," *Supercond. Sci. Technol.*, vol. 16, p. 24, 2003.

[18] D. M. Hwang *et al.*, "Application of a near coincidence site lattice theory to the orientations of YBa2Cu3O7-x grains on (001) MgO substrates," *Appl. Phys. Lett.*, vol. 57, no. 16, pp. 1690–1692, 1990.

[19] A. V. Pan *et al.*, "Enhancing properties of high-temperature superconducting step-edge Josephson junctions by nano-multilayers with a small mismatch," *Adv. Mater. Interfaces*, vol. 1, no. 3, Jun. 2014, Art. ID 1300112.